THE EFFECTS OF ENTRAINMENT ON THE HYDRAULIC EQUIVALENCE RELATIONSHIPS OF LIGHT AND HEAVY MINERALS IN SANDS[1]

RUDY L. SLINGERLAND
Department of Geosciences, Pennsylvania State University,
University Park, Pa. 16802

ABSTRACT: A semi-empirical critical velocity equation and critical suspension velocity equation have been developed to explain the settling velocity relationships and concentrations of light and heavy minerals in sands. Based on solutions to these equations and supporting experimental data, a fourfold classification of constant terminal settling velocity (CTSV) ratios of light and heavy minerals and heavy mineral concentrations has been constructed using ranges of R_*, the boundary Reynolds number, and d/BKS, the ratio of grain size in question to the bottom roughness grain size. If R_* is less than five and d_h/BKS is about one, a heavy enriched, well size-sorted, fine to medium size sand deposit should result, with entrainment equivalent size ratios of heavy to light grains up to four times smaller than those predicted by settling laws. If R_* is greater than five but less than 70 and d_h/BKS is about one, a fine to medium deposit should be formed of very heavy enriched, very well size-sorted sand, whereas if R_* is greater than 70 and d_h/BKS is less than one, a coarse more poorly sorted light mineral deposit should result. Garnet and quartz in heavy and light layers from a Presque Isle, Lake Erie beach have equal sizes in the heavy layers and equal settling velocities in the light layers as predicted. A beach heavy and light mineral size budget is proposed which incorporates these mechanisms.

INTRODUCTION

Hydraulic equivalence was first stated by Rubey (1933) as the assumption that "whatever the conditions may have been which permitted the deposition of quartz grains of a certain size, these conditions would also permit the deposition of magnetite grains (of a size) that had the same settling velocity." Using known settling velocity laws he deduced that the grain diameter ratios of hydraulically equivalent minerals in a deposit would be inversely proportional to a power of the ratio of their densities. Subsequent studies, however, have revealed the inapplicability of the hypothesis as exactly stated by Rubey; light and heavy minerals in most sands are not in hydraulic equilibrium in his sense of the terms (Lowright et al., 1972).

Explanations for deviations from hydraulic equivalence have followed two lines of reasoning as summarized by Lowright et al. (1972): 1) hydraulic inequivalence is the result of differ-

entially inherited size restrictions from the source rocks, or 2) hydraulic inequivalence is the result of differential transport of the various minerals in a sand. Rittenhouse (1943), van Andel (1950), Shanov (1964), and Briggs (1965) have presented data supporting the first line of reasoning. These data may be summarized by the work of Rittenhouse and Briggs.

Rittenhouse defined the hydraulic ratio of a mineral as "100 times the weight of a mineral in a known range of sizes, divided by the weight of light minerals of equivalent hydraulic size" (Rittenhouse, 1943, p. 1743). He measured hydraulic ratios for different sand sizes of the Rio Grande, showing that for the sands studied, the hydraulic ratio was lowest for the coarser sizes (0.25–0.175 mm). He interpreted this to mean that there existed a deficiency of larger sized heavies in the source rocks relative to larger sized lights.

Briggs (1965) documented that the modal separation between heavy and light settling velocities increased with increasing grain size for sample diameters larger than 0.125 mm.

[1] Manuscript received February 4, 1976; revised August 1, 1976.

He concluded that this reflected unrestricted size ranges available for the lights, as opposed to a restricted upper size limit for the heavies.

However, Feniak (1944) computed average grain areas from thin sections of 200 granitoid rocks in a study of the source size ranges of different minerals. The order of average area (estimated grain size) of minerals pertinent to this study is (largest to smallest): feldspars, pyroxene, olivine, hornblende, quartz, magnetite, sphene, and zircon. Thus it is not obvious that heavies always have smaller size distributions in the source, especially relative to quartz, as Briggs and others have assumed.

Subsequent work by Lowright et al. (1972) has shown that differential transport and not source restrictions can explain these observed deviations from hydraulic equivalence. They determined the settling velocity distributions of lights and heavies from Pleistocene tills (source), rivers, offshore sediments, and beaches and dunes in a complete sedimentary dispersal system near Presque Isle, Lake Erie. Their data show an equivalent range of sizes in the tills for the lights and heavies implying no source availability problem for the coarser heavies. However, in the Presque Isle beach and dune deposits after 20 miles of river and longshore transport, the largest and smallest heavies were no longer present. This was interpreted by them to indicate differential entrainment of the heavies versus the lights.

Differential entrainment of grains has been studied by von Engelhardt (1940), McIntyre (1959), Hand (1964), and Grigg and Rathbun (1969). Von Engelhardt determined from 14 modern dune and beach sands that the size distributions were explainable by a "process model" and that the influence of the source grain size distribution was slight. He demonstrated that the hydraulically equivalent sizes of quartz versus garnet and magnetite in suspension would be different from hydraulically equivalent sizes which were rolling.

Similarly, McIntyre hypothesized that smaller than predicted separations between quartz and garnet sizes from swash sands on Presque Isle were the result of selective removal of the coarser quartz by rolling.

Hand extended this idea to explain why heavy minerals in light layers on three New Jersey beaches had lower settling velocities than predicted by settling theory. He reasoned that because the heavies were smaller than the lights they would be shielded by the larger grains and also not protrude into zones of higher velocities. Thus the heavy that moves with a given light would settle slower than its larger hydraulically equivalent size, by an amount proportional to the degree of difficulty of entrainment. It is not apparent though, without invoking source size restrictions, why heavy grains should initially be smaller than the lights determining the bottom roughness.

Finally, Grigg and Rathbun (1969) showed again, that grains settled together will not necessarily be entrained together. Their analysis, however, used the Shield's criterion for the critical shear stress just needed to entrain sediment, which is not strictly valid for different sized grains in a sediment distribution.

Thus, deviations from hydraulic equivalence of light and heavy minerals in sands have been well observed, and differential entrainment has been investigated as a cause. However, no entirely adequate physical mechanisms have been proposed and no equations derived which can quantitatively predict the expected settling velocity distributions. This report presents quantitative theoretical and experimental support for deviations from hydraulic equivalence as a result of differential mineral entrainment. A critical velocity equation is developed which puts boundaries on the hydraulic equivalent sizes of light and heavy minerals in sands. The critical velocity concepts are then applied to the hydrodynamics of beach and foreshore light and heavy mineral deposition and tested with experimental data. As a result, a classification of heavy and light mineral settling velocity relationships and amount of heavy enrichment is proposed. Finally, in application to a natural system, the light and heavy minerals in beach foreshore deposits on Presque Isle, Lake Erie, are analysed in light of the theoretical and experimental data and a model is developed for the concentration of heavy mineral deposits in the beach foreshore zone.

THEORETICAL ANALYSIS

Velocity Profiles near Walls

The boundary velocity distributions used here are the Karman-Prandtl equations for the smooth and rough regimes of flow as defined by the boundary Reynolds number,

a   b
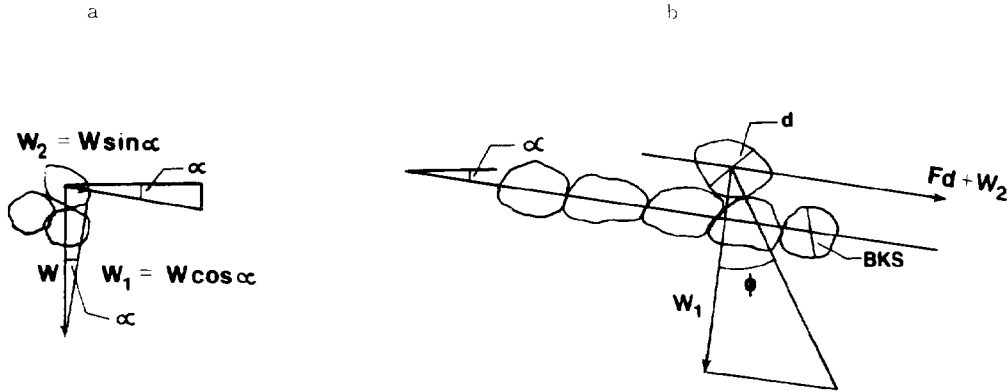
FIG. 1.—Force diagram for cohesionless particles of diameter d, on a bed of roughness BKS, slope α°. ϕ is the reactive force point angle.

R_*, which equals U_*BKS/ν where U_* is the friction velocity, BKS is a parameter describing the size of the roughness elements on the bottom, and ν is the kinematic viscosity. With the modifications of Einstein (1950) to include hydraulically smooth boundaries ($R_* < 5$), transitional ($5 < R_* < 70$), and rough boundaries ($R_* > 70$), the velocity distribution becomes:

$$V_y = 5.75 \; \log_{10}\left(\frac{30.2xy}{BKS}\right)U_* \qquad (1)$$

where V_y are mean point velocities at a high y from the bed datum, and x is a correction factor from Einstein (1950, Fig. 4).

Force Balance on a Grain on a Bed

Now consider a bed of loose cohesionless sand over which flows a fluid of uniform physical characteristics. For prediction of sediment transport, the forces to be considered are 1) inertial and viscous fluid drag forces, 2) fluid lift forces, and 3) reactive forces, the most important of which is the submerged grain weight.

Inertial force or form drag and viscous or surface drag are combined in the drag equation representing the force imparted to a stationary spherical particle within a moving fluid:

$$F_d = C_dA_p\frac{\rho_f V^2}{2} \qquad (2)$$

where: C_d = the coefficient of drag
A_p = the projected cross-sectional area of the particle

ρ_f = the density of the fluid
V = the fluid velocity on the grain.

The influence of lift is not considered in this study.

The reactive forces oppose the resultant of all active forces through the point of contact between a grain and the grains upon which it rests. The primary reactive force is the grain submerged weight which is assumed to act through the grain center of gravity, whereas the point of application of drag forces will vary with the grain shape and relative magnitudes of viscous to inertial forces. From Fig. 1a, the resolved submerged weight of a spherical grain on a slope of angle α is equal to:

$$W_1 = \frac{\pi d^3}{6}(\rho_p - \rho_f)g \cos \alpha. \qquad (3)$$

Parallel and down the slope is the resolved weight component of the grain:

$$W_2 = \frac{\pi d^3}{6}(\rho_p - \rho_f)g \sin \alpha. \qquad (4)$$

From Fig. 1b, the resolution of the forces about the reactive force point yields the condition of incipient motion:

$$\tan \phi \propto \frac{F_p}{F_n} \propto \frac{W_2 + F_d}{W_1} \qquad (5)$$

where: F_p = force parallel to slope
F_d = down slope drag force
F_n = force normal to a slope inclined α degrees.

This is a two dimensional balance of moments at the grain centroid and at the reactive force

point and does not consider frictional forces between adjacent particles.

Substituting equations 2, 3, and 4 in 5, one obtains for incipient motion of a spherical particle of diameter d on an equidimensional bed of diameter BKS:

$$\tan \phi \propto \frac{3C_d V^2 \rho_f}{4dg \cos \alpha(\rho_p - \rho_f)} + \tan \alpha. \quad (6)$$

The critical velocity may be defined as the fluid velocity at which sediment particle motion commences, measured at 'y' units from a datum on which the surface sediment rests. Solving equation 6 for Vc, yields:

$$Vc \propto \sqrt{\frac{4dg \cos \alpha(\rho_p - \rho_f)(\tan \phi - \tan \alpha)}{3C_d \rho_f}} \quad (7)$$

Since Vc is the critical velocity of a grain of diameter d, on a bed of roughness BKS, Vc, as a first approximation can be made equal to $U*$, the boundary friction or shear velocity. In other words, the needed transport energy represented by a velocity, Vc, must equal the amount of energy lost to transport, represented by $U*$. This is not strictly true since according to Chezy for open channel flow (Leliavsky, 1966):

$$\tau_o = C^2 V^2$$

or:

$$V = \sqrt{\tau_o/C^2} = \sqrt{U*^2 \rho_f/C^2} = \frac{\sqrt{\rho_f}}{C} U*$$

where: V = mean fluid velocity
τ_o = intensity of tractive force of moving water per unit area of bed,
C = Chezy C.

But since $C = 1.49 R_h^{1/6}/n$, and the variation of these parameters is of small order of magnitude compared to the range of the variables of interest, the approximation is assumed to be valid.

Thus, combining equations 1 and 7 yields:

$$Vc \propto 5.75 \log_{10}\left(\frac{30.2xy}{BKS}\right)$$
$$\sqrt{\frac{4dg \cos \alpha(\rho_p - \rho_f)(\tan \phi - \tan)}{3C_d \rho_f}} \quad (8)$$

which is the critical erosion velocity measured at a height y from the bed datum.

Some Additional Assumptions

In addition to the already stated and generally accepted assumptions, these implicit assumptions have been made. 1) The relationship $\tan \phi \propto F_d/F_n$, is an assumption that $F_d = f(\tau_o A_p)$ since the force about the reactive force point is actually due to a torque from an applied shear stress. 2) Theoretically, the velocity term in equation 8 is the fluid velocity impacting on the cross-sectional area of a sphere free from wall effects, and may be functionally related to Vc.

Equation 8 includes the C_d which many investigators take to be constant. The increase in drag on smaller sized particles will cause a reduction in Vc for which the C_d will account. Although the general Cd vs. Re curve was developed for a sphere falling freely through a fluid, it has been shown that the dynamics of the drag force caused by water on a sphere resting on a surface is similar (Coleman, 1967).

Quantification of Sediment Parameters

Equation 8 represents the readily quantifiable parameters relevant to sediment transport. Before application to a natural system, the following more complex variables must be accounted for: random turbulent velocity fluctuations, grain shape, the point of application of the drag forces, packing, cohesiveness, and quantification of the reactive force angle.

Kalinske (1943, p. 274) found that, "fluctuations equal to twice the mean velocity at a point in the turbulent zone near a boundary can be readily expected." Similar measurements by Grass (1967) confirm that as the flow regime passes from the transition zone into the hydraulically smooth regime with a viscous sublayer, it is reasonable that the turbulent velocity fluctuations at the level $y = BKS$ (cf. Yalin, 1972, p. 98) will decrease and become negligible. There is no theoretical reason why this decrease should not be continuous, and as a first approximation, a coefficient β_1 will be introduced to account for the variation in critical velocity due to turbulence. β_1 will equal 0.5 at $R* > 70$, increasing to 1 at $R* < 5$. Thus from the equation for a straight line:

$$\beta_1 = -0.0077R* + 1.038 \quad (9)$$

for $5 < R* < 70$.

For mathematical simplicity, grain shape has been assumed to be spherical. In this study quartz and garnet were used because they were reasoned to be subequant and nearly identical in shape characteristics.

The point of application of the fluid forces can be reasoned to be some function of the ratio BKS/δ', the size of the roughness elements to the thickness of the viscous sublayer, since increased immersion in the viscous sublayer will increase viscous forces which tend to raise the point on the grain through which the force acts. Experimental data from White (1940) indicate that for small BKS, $\alpha\eta = 0.37$ where α is a coefficient reflecting the point of application of fluid forces and η is a packing coefficient. Since small BKS implies close packing or $\eta \approx 1$, α must be on the order of 0.3 to 0.4. Since BKS/δ' is proportional to $R*$, a second coefficient β_2 is defined as:

$$\begin{array}{ll} \beta_2 = k_1 & R* < 70 \\ \beta_2 = k_2 & R* > 70. \end{array} \quad (10)$$

In this study the packing coefficient is assumed to be constant and equal to 1.0.

Below $d = 600\ \mu$ sediment may exhibit both frictional and cohesive properties (Sundborg, 1956). However, for sediment in the size range composed mainly of sand, Grass (1970) has shown that for d down to 50 μ the critical velocity curve can be expected to flatten but still decrease for decreasing grain size where grain cohesion is not an important property.

For noncohesive sediments, the wide range of grain sizes and possible combinations of grains in contact with each other will yield a wide range of reactive force angles. This angle, ϕ, according to Miller and Byrne (1966), or Ippen and Eagleson (1955), can be defined by:

$$\tan \phi = \frac{0.866}{\left(\left(\dfrac{d}{BKS}\right)^2 + 2\left(\dfrac{d}{BKS}\right) - \frac{1}{3}\right)^{1/2}} \quad (11)$$

for the most likely path of rolling of a grain, where d, BKS, and ϕ are defined in Fig. 1. It has been found that allowing $BKS = d_{65\%}{}^2$ in equation 11 yields for measurements made on natural sands a spread of values around 28 degrees, the exact value of which depends on

the sorting of the size distribution and the grain size in question.

Substituting the preceding coefficients into equation 8 gives the final approximation of the critical erosion velocity needed for a particle of size d on a bed of roughness BKS:

$$Vc = \frac{5.75\ \log_{10}\!\left(\dfrac{30.2xy}{BKS}\right)\beta_1\beta_2}{\sqrt{\dfrac{4dg\ \cos\ \alpha(\rho_p - \rho_f)(\tan\ \phi - \tan\ \alpha)}{3C_d\rho_f}}} \quad (12)$$

where: $\tan\ \phi$ = reactive force angle (equation 11)

C_d = coefficient of drag

x = Einstein correction factor (Einstein, 1950, Fig. 4)

BKS = roughness size = $d_{65\%}$

α = bed slope in degrees

d = grain diameter

g = gravitational acceleration

ρ_f = density of fluid

ρ_p = density of particle

β_1 = turbulent velocity fluctuation coefficient

β_2 = coefficient for point of application of fluid force.

Solution of the Equation

Equation 12 as presented is not readily solvable since the Vc is a function of the coefficient of drag, which is a function of the fluid flow around the grain. The solution to the equation is obtained by using the Schiller equation (1933, *in* Graf, 1972), relating the coefficient of drag to the Reynolds number for a falling sphere:

$$C_d = \frac{24}{Re}(1 + 0.15Re^{0.687}). \quad (13)$$

We may define a critical Reynolds number as:

$$Re_c = \frac{V_c\ d}{\nu} \quad (14)$$

Substitution of equation 14 in 13 and 13 in 12 gives a complex polynomial in Vc which may be solved by the Newton-Raphson Method (James et al., 1967, p. 139).

Comparison of Theoretical with Experimental Results for the Critical Velocity Equation

We must now evaluate the assumptions in the previous section and the correctness of the

---

[2] $d_{65\%}$ is defined as that grain size for which 65% of the distribution is finer.
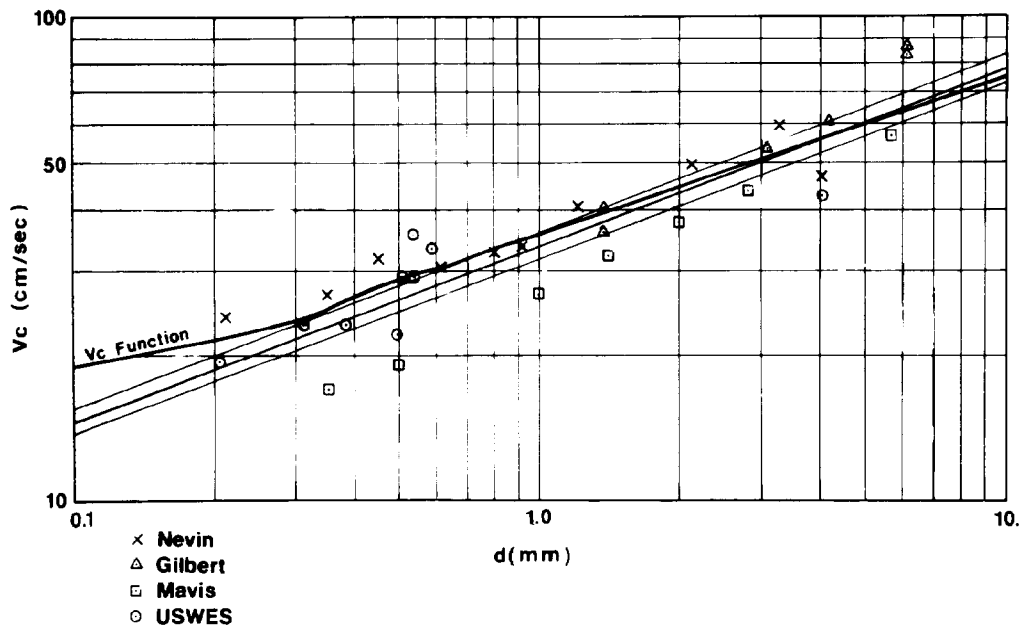
FIG. 2.—Plot of the Vc function from this report for 1-cm depth, with experimental values from Nevin (1946), Gilberg (1914), Mavis (1935), and United States Waterways Experiment Station (1935). Included is the simple linear regression equation for the data: $Vc = \log_{10}Vc = 1.53 + 0.36 \log_{10}d$, with the 95% confidence limits on the Vc intercept.
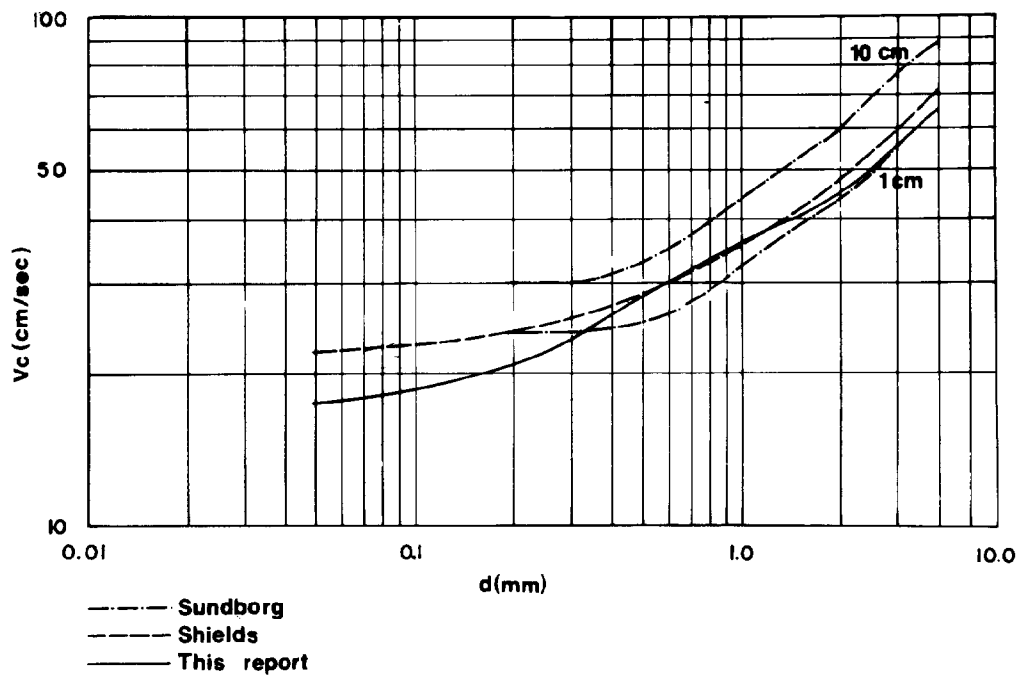
FIG. 3.—Plot of the Vc function from this report with those of Sundborg (1956) and Shields (1935 in Grigg and Rathbun, 1969). The Sundborg plots are for a depth of 1 cm and 10 cm as labeled.
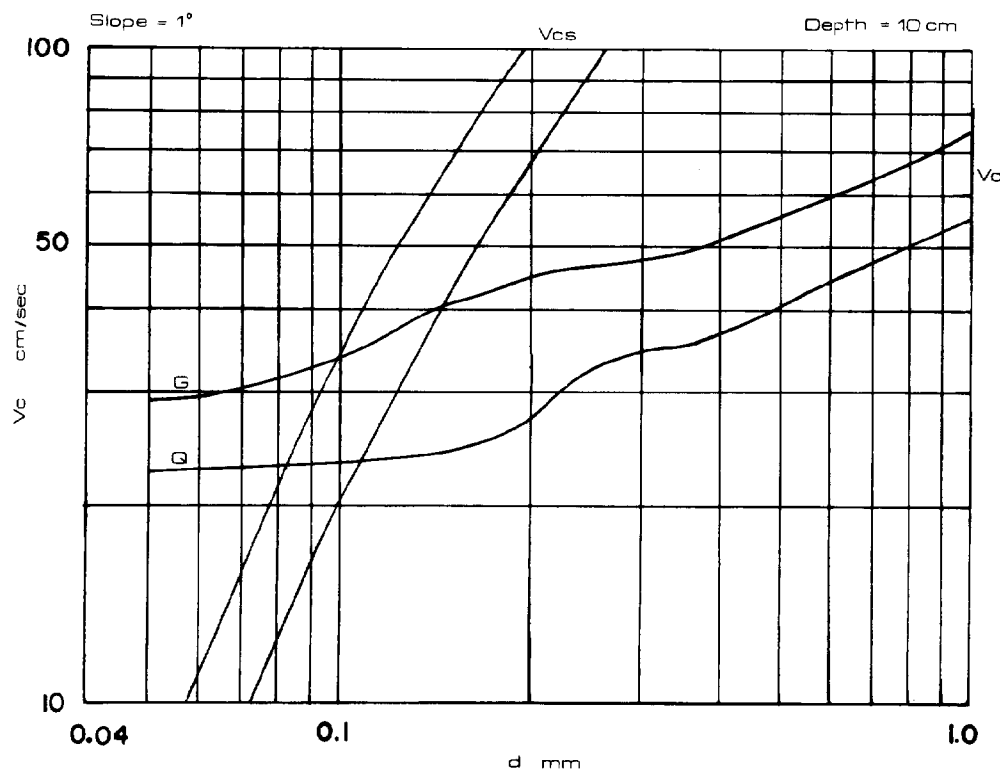
FIG. 4.—Plot of the critical velocity (*Vc*) and critical suspension velocity (*Vcs*) equations vs. grain diameter for quartz (Q) and garnet (G), for depth = 10 cm, slope = 1°.

β_1 function as well as determine the constants of β_2. Figure 2 shows the *Vc* function with experimental data from Nevin (1946), Mavis (1935), Gilbert (1914), and USWES (1935), recalculated to standard conditions of 1-cm depth, $\rho_p = 2.65$, $\rho_f = 0.9979$, slope = 0.0004, and $BKS = d_{85\%}$ of the bottom size distribution. This fit is with $\beta_2 = 0.3$ for $R* < 70$ and $\beta_2 = 0.33$ for $R* > 70$. These values are commensurate with expected values of 0.3–0.4 as discussed in the section on quantification of sediment parameters. Also, for uniform sediments, β_1 was best estimated as $(f(Re))^{1/2}$ thus limiting its variation from 0.71 to 1.0 over the range $R* = 5$ to 70.

Figure 3 is a plot of the *Vc* function (equation 12) with the entrainment functions of Sundborg (1956) and Shields (1935, *in* Graf, 1972). Equation 12 predicts lower values for the finer sizes (<0.4 mm) than either of the other two equations as a result of the influence of the increasing value of C_d at lower Re_c. Figure 2 indicates that the linear regression line of the experimental data actually predicts lower *Vc* values for the smaller sizes down to 0.2 mm than the entrainment function. The entrainment function $(V_c = f(d))$ is at least as accurate in predicting *Vc* values for this range as the Shields and Sundborg functions. Above 0.6 mm the entrainment function maps within the 95% confidence limits of the regression line for the experimental data.

Critical Suspension Velocity

The critical suspension velocity is herein defined as the mean fluid velocity measured at a distance *y* from the bed, which just maintains suspension of a particle of constant terminal settling velocity (*CTSV*) *Vs*, where *Vs* is the settling velocity of the particle in still water. Experimental evidence from Lane and Kalinske (1939, p. 640), indicates that *U*∗ must be greater than or equal to *Vs* to initiate suspension of a particle of *CTSV*, *Vs*. As previously mentioned, *U*∗ can be seen to be a function of the intensity of the turbulent

100

50

Vc(cm/sec)

BKS = 0.3

BKS = 0.2

BKS = 0.09

10

0.04

0.1

1.0

d(mm)
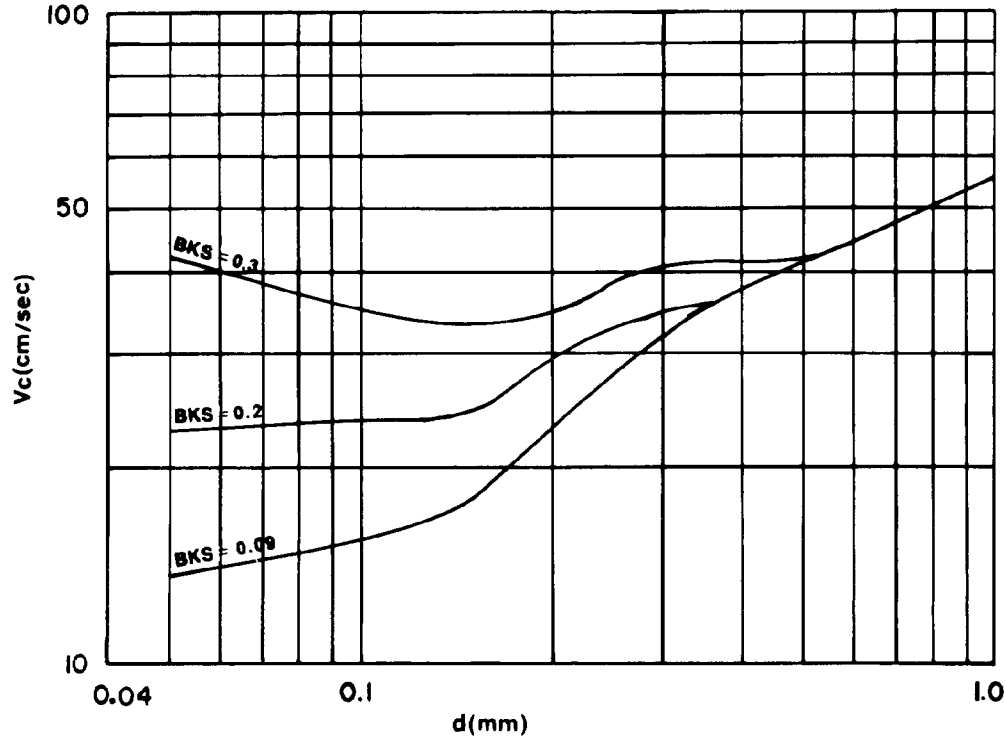
Fig. 5.—Plot of Vc function vs. grain diameter for three different bed roughness sizes (BKS) in mm, with density = 2.65, slope = 7°, and depth = 10 cm.

velocity fluctuations. It is then reasonable to assume that $U*$, as a measure of the vertical velocity components of the turbulent flow, would have to equal Vs, for suspension. Substituting Vs for $U*$ in equation 1 yields:

$$Vcs = 5.75 \log_{10}\left(\frac{30.2xy}{BKS}\right)Vs \qquad (15)$$

where Vcs is the critical suspension velocity which is dependent on the point of measurement, the boundary roughness, and the $CTSV$ of the particle in question. This allows comparison of horizontal flow velocities needed to maintain suspension of a particular sized particle with that velocity needed for entrainment.

REPRESENTATIVE SOLUTIONS OF THE CRITICAL VELOCITY EQUATIONS

Figure 4 is a solution of the Vc entrainment and suspension functions for a depth of 10 cm (the point of measurement), grain densities of quartz and garnet, $BKS = d$, and bed slope = 1°. The form of the entrainment function varies for different densities, in contrast to

the usual representation of the Vc equation as displaced parallel curves. This form difference is a result of the higher $U*$ needed for denser grains. The relationship between Cd and $R*$ changes, thus changing the form of the function.

Figure 5 is a plot of Vc vs. d (mm) for three different ϕ roughness sizes equal to 0.09, 0.2, and 0.3 mm with $\rho_p = 2.65$ and water depth = 10 cm. The increase in size of the bed upon which a grain rests causes an increase in Vc for all sizes up to 0.25 mm larger than the given roughness size. With a ϕ roughness size of 0.3 mm the increase in Vc is greater for the smallest grains decreasing to 0.15 mm after which it increases again becoming equal to Vc for a ϕ roughness size of 0.2 mm at d = 0.55 mm. For a ϕ roughness size of 0.09 mm, the decrease in Vc is especially great for the smaller sizes since the grains no longer are hidden amongst larger grains which cause larger ϕ angles.

Figure 6 is a plot of the Vc function vs. grain size for $\alpha = 7°$, depth = 1 cm, $BKS = 0.2$
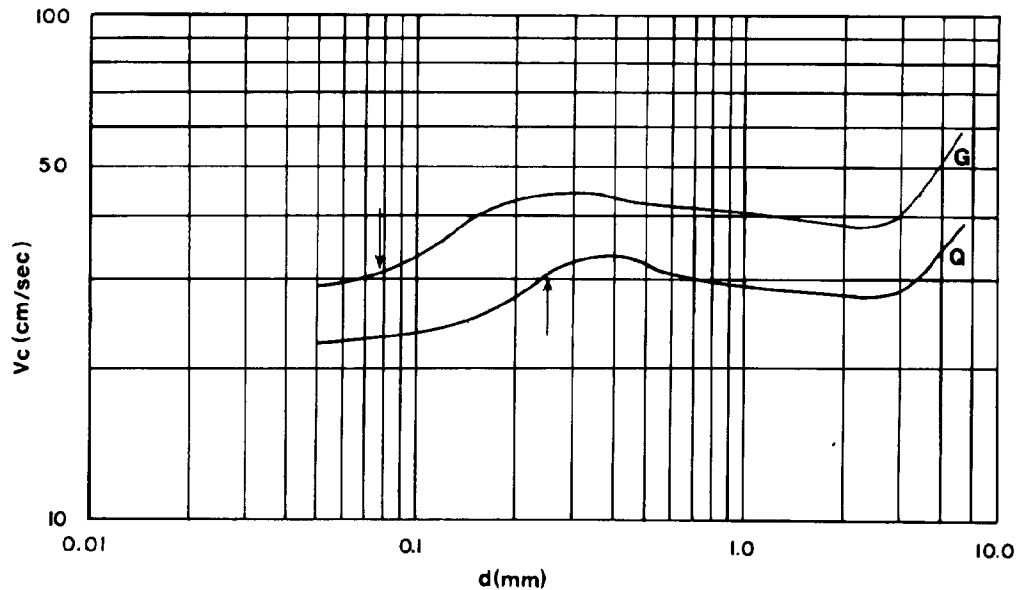
Fig. 6.—Plot of the Vc function vs. grain diameter for quartz (Q) and garnet (G) with the slope = 7°, depth = 1 cm, where ϕ is unrestricted to 3°.

mm, and where ϕ is unrestrained to 3°. This is assumed to reflect the situation where grains of a wide range of sizes are resting on a bed of fairly uniform smaller grains on a steep slope, for example, an upper beach swash face. The form of the function indicates that in this situation some grains larger than about 0.35 mm are easier to entrain than smaller grains. The function is of this form because between $d = 0.15$ to 3.5 mm, the decrease in Cd for increasing Re offsets the variation of ϕ and β_1, causing higher critical velocities. As Cd approaches a constant value, the decrease in ϕ and β_1 balances the increase in force needed to move grains of larger size and the critical velocity decreases slowly.

EXPERIMENTAL DATA

Water Table Studies

A recirculating water table usually used for aerodynamic shock-wave studies was modified for observing the relative transportation rates of sand-sized heavy and light minerals. The table consisted of a 1.5 meter wide plate glass surface of slope = 0.001, at the upper end of which was a metal plate with a uniformly beveled lower edge. By rotation of the plate about its upper edge, the velocity and type of flow over the table bottom could be

regulated. Because of the table construction, the flow should approach the theoretical case where a viscous sublayer exists at the bed, becoming turbulent above.

The grains used were monomineralic natural populations size to $\frac{1}{4}\phi$ intervals. At the beginning of a test, 1.5 g of each sieve fraction were placed along a line parallel to the flow regulation gate. Flow of the water was increased to 0.66 m/sec (depth = 2–4 mm at 0.3 m downcurrent from the gate), and held at this velocity for approximately one minute, whereupon the flow was stopped. The distances of movement downcurrent of the various size fractions were measured.

Figure 7 is a plot of the Vc function and the observed distance of movement of the various fractions for quartz and garnet (some experimental data from James Warg, personal communication). Although the distance moved is taken to be proportional to the Vc for a given size sediment, the position of the curves on the graph is arbitrary, thus only the relative forms of the curves are meaningful. The close agreement between the predicted and observed critical velocities supports the theoretical conclusions of this report at least for the ideal case, concerning the variation in Cd, β_1, β_2 and ϕ. The viscous flow over the smaller
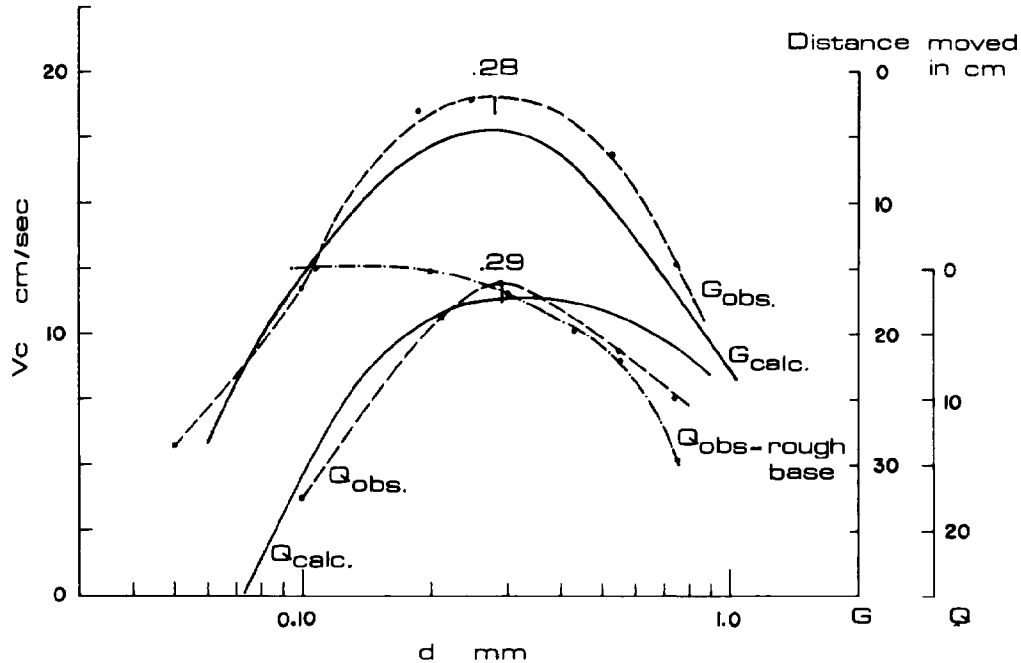
FIG. 7.—Plots of the calculated Vc function (calc) and observed distance of movement (obs) vs. grain diameter for quartz (Q) and garnet (G). Also plotted is the observed distance of movement of quartz grains on a rough base, with BKS = 0.102 mm (Q_{obs} – rough base).

grains will create more drag and hence a larger Cd than for larger grains. Larger grains, however, will experience higher turbulent velocity fluctuations, a higher point of application of fluid force, and larger ϕ angles. Thus there will be some relationship between Cd, β_1, β_2, and ϕ angle where the force imparted to a grain is at a minimum. This is the size for which the Vc must be highest in Fig. 7. The size least easily moved is not the largest or smallest but some intermediate size, depending upon the sediment and fluid conditions.

This conclusion is contrary to the generally accepted Vc size relationship as presented in Hjulstrom (1935) and Inman (1949) who showed 0.18 mm to be the size most easily entrained. But the Hjulstrom data are a mixture of Vcs for cohesive clays as well as fine sands. In that case the Vc will increase below 0.18 mm. Also, the analysis of Inman that the redistribution of drag at $R*$ < 5 (0.18 mm size at standard conditions) will cause an increase in the Vc is contrary to the data of Grass (1970) and this report. Finally, neither Inman or Hjulstrom analyzed explicitly the differences in Vc owing to variations in ϕ as a result of specific differences in size distribution.

With a Rough Base

To determine the degree of deviation from ideal conditions, the glass plate bottom of the water table was replaced with a plate upon which sand of uniform size (0.104 mm) had been glued. The quartz curve for a typical run under these conditions is superimposed on Fig. 7. As predicted from Fig. 5, grains with diameters up to 0.25 mm greater than the base roughness size had ϕ angles increased and velocity gradients reduced so that their Vc exceeded the fluid velocity. Therefore no grain movement occurred with grain diameters less than 0.20 mm.

Wave Tank Studies

These experiments were conducted in a wave tank 0.32 m deep, 1.2 m wide, and 4 m long. One end contained a dislocation-type wave generator; on the opposite end was located a gradually sloping beach of quartz sand.
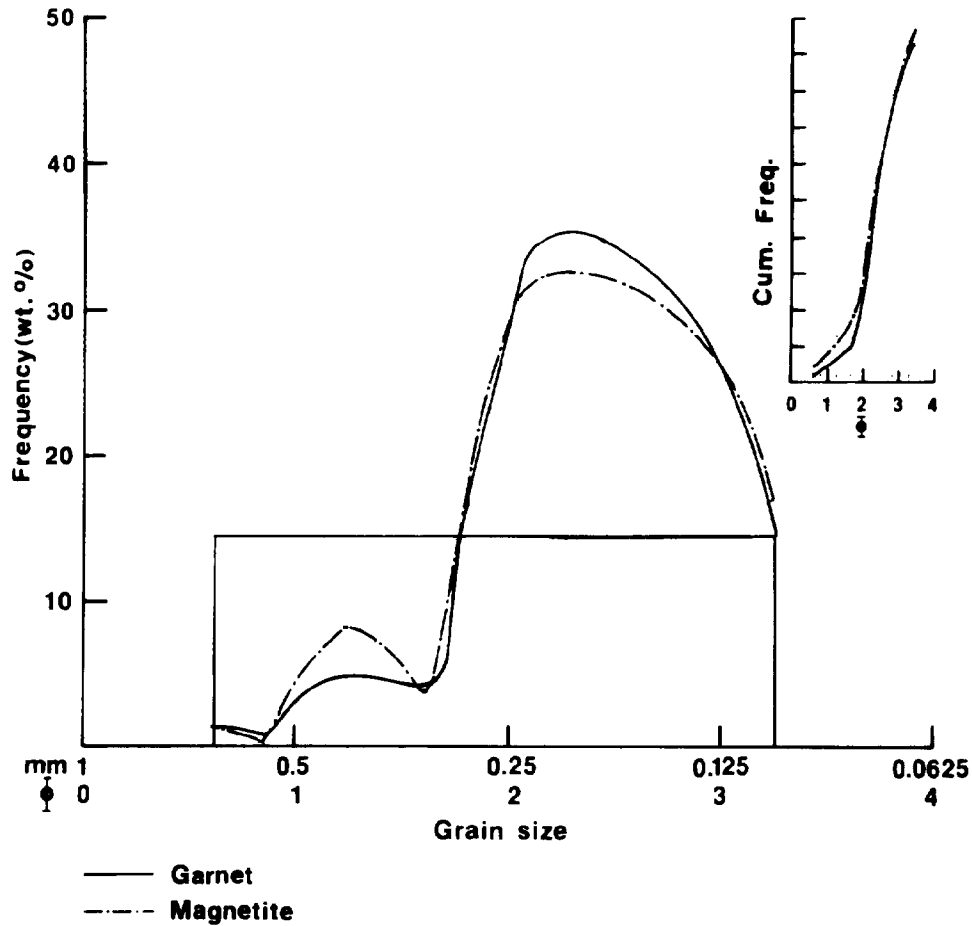
FIG. 8.—Frequency-grain size and cumulative frequency-grain size plots of garnet and magnetite for Run 1. Initial distribution is rectangular; swash modified distributions are bimodal.

In the first set of experiments, rectangular distributions (sizes 0.888 to 0.707 mm) of garnet and magnetite (run 1), and quartz, garnet, and magnetite (run 2), were introduced on the beach of bed size 0.22 mm. Samples of run 1 were located about ⅔ of the way up the swash face under destructive wave conditions, and the samples from run 2 were located immediately under the plunge point of the waves under constructive conditions. After 27 waves had passed, the remains of the initial samples were resampled and dried. The garnet and magnetite were separated from the quartz by heavy liquids, and the magnetite from the garnet by magnetic separation. All fractions were sieved and weighed. Figures 8 and 9 give the frequency distributions and cumulative weight percent curves for the various samples and runs.

In all the runs the larger sizes (0.324 to 0.707 mm) were selectively removed and always the minerals were removed by an amount inversely proportional to their densities. Figure 6 predicts for quartz that sizes from 0.3 to 0.5 mm will be harder to entrain than from 0.5 to 0.7 mm which is verified by the minor mode in Figs. 8 and 9. Combining a BKS between 0.2 and 0.3 mm from Fig. 5 with Fig. 6 will also produce the situation experimentally observed in Fig. 7 (quartz observed, rough base) which is additionally verified in Figs. 8 and 9. Also, from run 2 for samples at the plunge point, less of the larger sizes and more of the finer sizes were removed, possibly indicating that be-
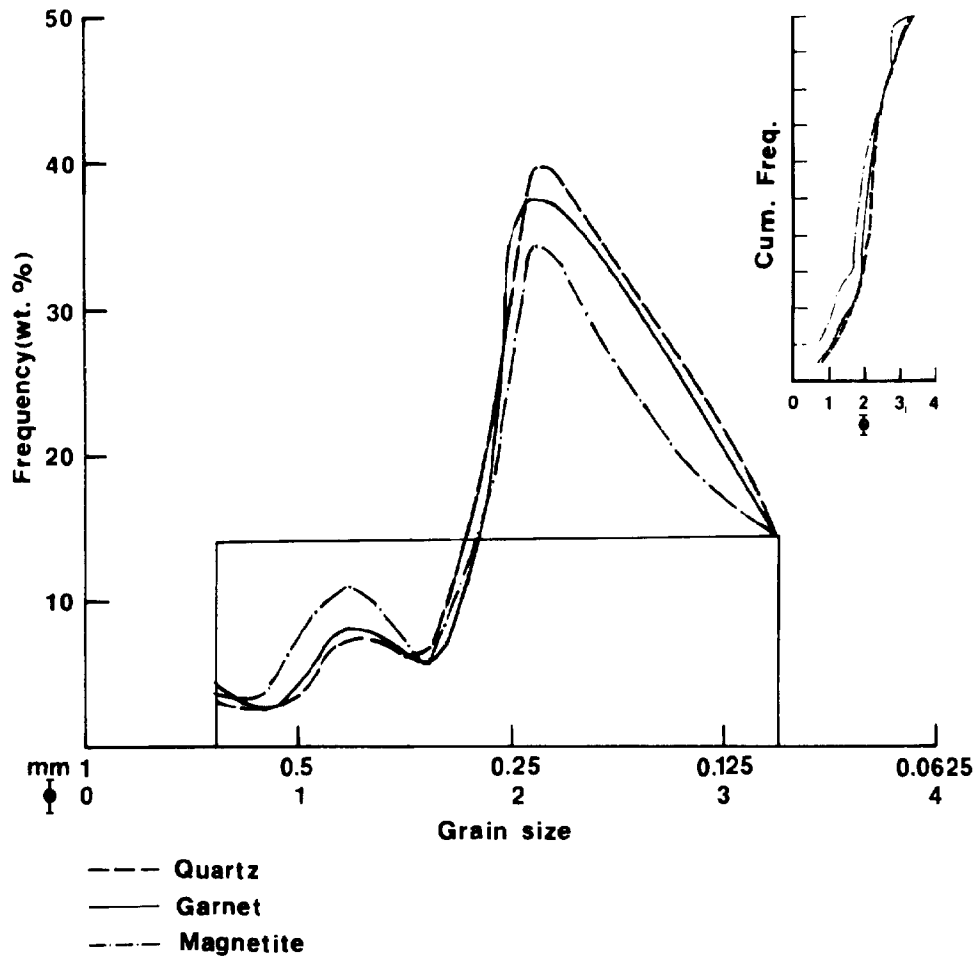
FIG. 9.—Frequency–grain size and cumulative frequency–grain size plots of quartz, garnet, and magnetite for Run 2. Initial distributions are rectangular; swash modified distributions are bimodal.

cause of the greater $R*$ and the increased turbulence, the smaller grains were plucked out from between the larger grains by a vertical velocity component.

SHE Distributions of Quartz and Garnet

To test the influence of the roughness size in the swash zone on transportation of SHE sized grains, equal amounts by weight of standard hydraulically equivalent (SHE) garnet and quartz (sieve sizes 0.148 and 0.210 mm, respectively) were introduced on an artificial base of sand cemented to plexiglass. Eight swashes passed over the samples, which were then re-

sampled, dried and weighed. Three different base roughness sizes were used; all were well sorted. The data are presented in Table 1. The increase in the relative proportions of quartz to garnet is an indication of the change from where the boundary roughness was such that the larger quartz could roll away to the situation where the finer heavies were entrained by fluid turbulence.

DISCUSSION

Based upon this theoretical analysis and experimental data, a model of heavy mineral selective sorting may now be proposed. As grains move over a given area of the bed, they
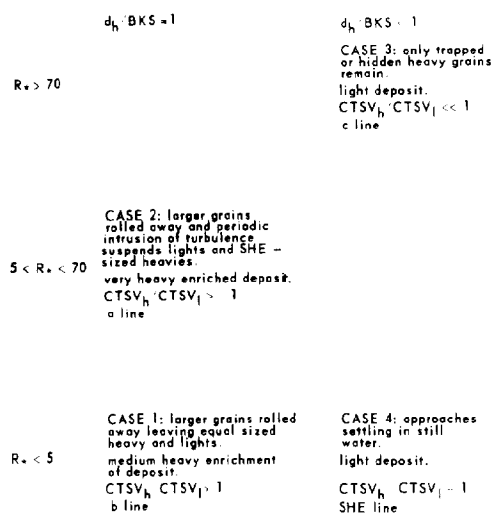
FIG. 10.—A classification of sediment-fluid conditions controlling the relationships of light and heavy minerals in sands.

FIG. 11.—*CTSV* garnet/*CTSV* quartz ratio lines as given in Fig. 10 plotted with samples from Presque Isle, Pennsylvania and Avalon, New Jersey.

test the flow and interparticle geometry for stable positions. Given a certain bottom roughness and current velocity, Figs. 5, 6, and 7 show that the size already established on the bed will select like-size particles in preference to larger and smaller sizes. Thus the tendency here is to minimize the effect of hydraulic equivalence by settling and select only by size, since β_1, β_2, and ϕ are determined predominantly by size.

However, from Fig. 4, the frequency with which grains of a certain density will test conditions on the bed is a function of the Vcs. Heavier grains of a given size will test the bed more than lighter ones of the same size, and thus have a better chance of filling a position. Also, from Fig. 4, if a heavy grain and a light grain happen to have the same ϕ angle, their hydraulically equivalent entrainment sizes will be quite far apart. These processes then emphasize density. Thus two different

TABLE 1.—*The relationship between base roughness and quartz/garnet ratios*

Wt. Qtz. / Wt. Gnt.	Base Roughness
0.656	0.149
0.823	0.190
1.13	0.210

controls—one depending on size, and one on density—are attempting to differentiate the sediment.

The variables exerting this control are functions either of the d/BKS ratio or a measure of the fluid flow at the bed. It is reasonable then, to use d/BKS and a $R*$ to classify the $CTSV$ relationship of light and heavy minerals in sands. Figure 10 shows the combinations of these two parameters thought to be important.

Case 1.—$R* < 5$ and the roughness size of the bed is nearly the same as the median size of the immediately available heavies ($d/BKS \sim 1$). As argued above, selection of heavy and lights is more by size than density. Thus the population will tend towards equal-sized heavy and lights because the hydraulically equivalent larger lights have lower critical velocities due to lower ϕ angles and greater turbulent influences from outside the viscous sublayer. Heavy enrichment has now occurred by rolling away the larger sized lights even though they are hydraulically equivalent in Rubey's sense of the term to the remaining heavies. This case is represented by the b line of equal *sized* heavy and lights in Fig. 11.

Case 2.—$5 < R* < 70$, but at the lower end, and $d/BKS \sim 1$. Case 1 entrainment

Study area   a   b

Penna.

berm

plunge pt

N   20ft.

LE-18   LE-19   LE-20   LE-14   sample no.
89.8   86.9   3.1   91.4   wt. % heavies
217.5   216.2   263.7   224.4   quartz
214.6   199.3   189.9   213.3   garnet   mean c axis, μ

LE-17   LE-16   LE-15
89.4   1.4   93.7
233.6   317.8   201.2
225.6   209.5   195.2

c

2ft.

X   X'
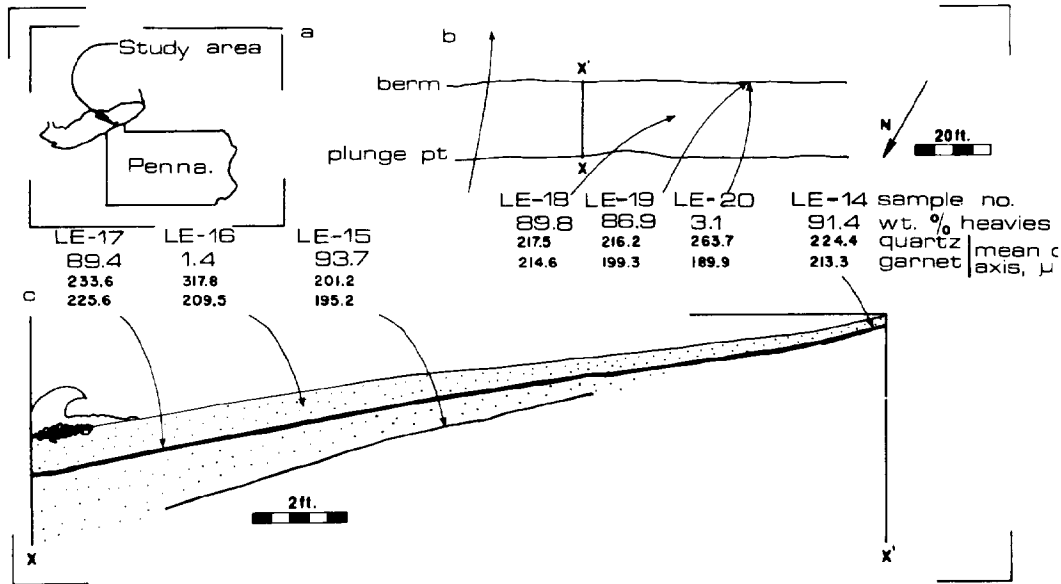
FIG. 12.—Location of study area (a); plan view of Presque Isle beach #10 in September, 1972 showing sample sites (b); cross section X–X' from b (c).

mechanisms will attempt to produce a uniformly sized heavy and light deposit, but in addition, periodic intrusion of turbulence from above into the viscous sublayer will suspend the lights and smaller (suspension equivalent) heavies. The deposit will then consist of a well size-sorted, even more heavy enriched population. The heavy grains now are equal to or larger in size than the lights because the light grains, if present at all, are trapped in the heavies. Although this case would produce $CTSV_h/CTSV_l$ ratios anywhere above the b line in Fig. 11, line a is chosen as representative of this situation.

Case 3.—$R* > 70$, and median size of heavies is smaller than the roughness determining population ($d/BKS < 1$). Only entrainment equivalent heavy sizes or heavies that are small enough to lodge within the larger population will remain, since fluid turbulence will act to remove all suspension equivalents. If the bed conditions were those of Fig. 6 for example, with $BKS = 0.2$ mm and median size of garnet about 0.07 mm, the entrainment equivalent sizes of quartz would be 0.25, 0.7, and 4.8 mm. Taking the first case gives a $CTSV_g/CTSV_q$ ratio of 0.8/3.33 which is much less than 1. The other two entrainment equivalent sizes and the case of trapped

heavy grains produce ratios smaller than this. Therefore line c is drawn through the point (0.8/3.33) to illustrate Case 3 ratios.

Case 4.—$R* < 5$, $d/BKS < 1$, or the fluid velocity is sufficiently small for fluid conditions to approach still water. This is represented in Fig. 4 by all diameters to the left of the Vcs line. This case is represented in Fig. 11 by the standard hydraulically equivalent (SHE) line, which may also represent the set of entrainment conditions such that the Vc of the heavy and light grains produces SHE sizes.

APPLICATION TO NATURAL SYSTEMS

The preceding theoretical and experimental development will now be tested on the nearshore-beach-dune complex of Presque Isle, Lake Erie. Samples of heavy and light mineral layers were collected in September 1972 from existing beach and dune deposits. Figure 12 gives the sampling locations, percent heavies, and mean c axial lengths.

The sampling procedure was designed to obtain single sedimentation unit samples by minimizing the thickness to a few mm. One half of each sample was dried, weighed and the heavy and light fractions separated by heavy liquids. The weight percent of heavies and lights was then calculated. To measure

grain size, the other half of each sample was split with an Otto microsplit until a quantity small enough to mount on a gelatinous-coated slide was obtained. Slide points were chosen by determining stage coordinates selected from a random number table. The apparent a and c axes of the five quartz and garnet grains closest to a point were then measured using a microscope with a 10× objective for a total of 50 grains per slide.

A multivariate discriminate function on both the a and c axes was used for comparison of the mean sizes of the lights and heavies. It finds the greatest distance between the two clusters (garnet and quartz) of multivariate points (a and c axial lengths) such that each cluster also has the least inflation (multivariate variance). Limited departure from normalcy does not seriously affect the function but the means and variances of the axes must be independent. This was shown to be fulfilled for these samples (Slingerland, 1973).

A measure of the separation between the two multivariate means, Mahalanobis D^2, may be tested for significance by an F test. The null hypothesis is that the two means are equal, or that the distance between them is not significantly different from 0. The F value at the 95% level of significance is 3.2 with $\nu_1 = 2$ and $\nu_2 = 92$. Figure 13 is a plot of the F values for D^2 for the samples collected.

There is no statistical difference between the multivariate means of the a and c axes between quartz and garnet of the samples from heavy layers (numbers 14–15 and 17–19). When the converted $CTSV$s calculated from the mean c axial length are plotted in Fig. 11 they fall on or near the b line, as is consistent with the postulated conditions of Case 1 (Fig. 10). The light layers (samples 16 and 20) plot along the SHE line, indicating that the heavies were not trapped but apparently were deposited under fluid conditions allowing suspension equivalent sizes to come to rest together. In addition, after settling, the BKS and fluid flow conditions must have been such that $R_* < 70$ since entrainment of the smaller sizes did not occur. Neither was R_* small enough to cause removal of the larger lights by rolling. Also plotted in Fig. 11 are three samples from light layers at Avalon Beach, N.J. (data from Hand, 1964) illustrating that even at smaller sizes, the $CTSV_h/CTSV_l$ ratios fall as predicted.
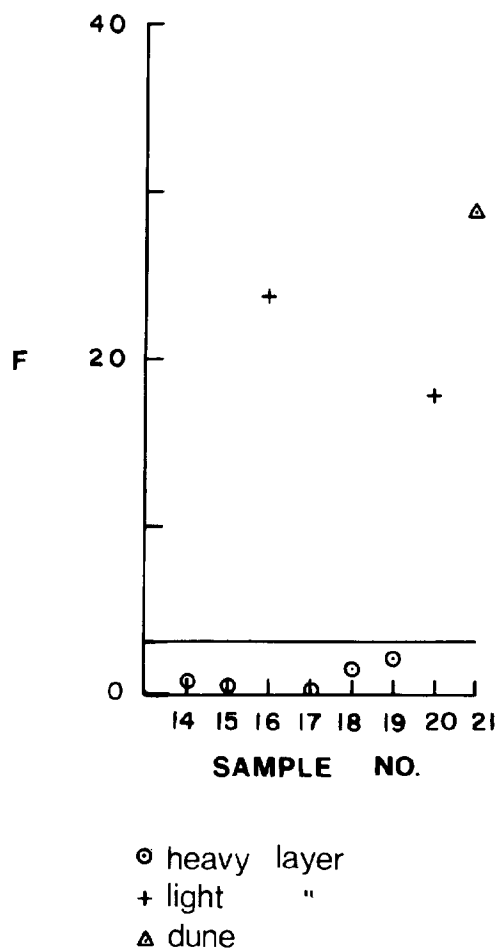
FIG 13.—F test values on Mahalanobis D^2 for Presque Isle samples; F significance value at 95% confidence level = 3.2.

Heavy and Light Mineral Budget for a Presque Isle, Lake Erie Beach

Results of this paper plus those of Lowright et al. (1972) may now be used to construct a heavy and light mineral size budget for the Presque Isle beach. Modification of the ultimately available sizes has already occurred by the time the sands have reached the lake bottom offshore from the beach, producing the settling velocity distributions in Fig. 14 at point y.

Deposition in the swash zone of sizes from these distributions will proceed in the following manner. SHE sizes in suspension (aa) and
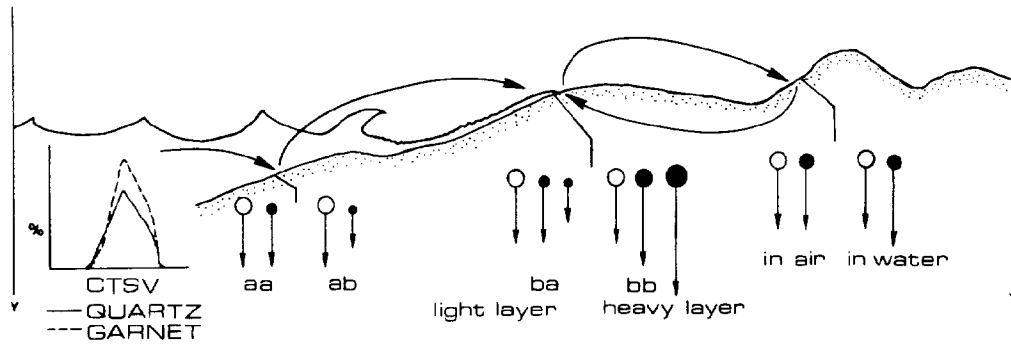
FIG. 14.—Schematic heavy and light mineral size budget for Presque Isle beach.

entrainment sizes in saltation (ab) with *CTSV*s between SHE and the c line will settle out up the beach face in proportion to the decrease in velocity with the coarser sizes settling first. Because the swash must decrease to 0 velocity, and given the average order of magnitude of swash velocities on sandy beaches, the top of the swash is the most likely place to have a fluid velocity and grain size such that $R* < 70$, which may even approach $R* < 5$. (For $R* = 70$ and with a grain size of $BKS = 0.7$ mm, the V at 1 cm depth $= 161$ cm/sec.). Also because the distribution of sizes will settle out according to equation 15, the upper portion of the swash will contain the finest sizes of the population and thus the *BKS* grain size may be of the same order of magnitude as the size of the heavies. As deduced in a previous section this represents optimum conditions for the enrichment of heavy minerals, since all larger-sized grains may be rolled away. Consider now, the fact that some swashes will be higher than others, and will thus produce a higher than usual velocity for a point near the top of the swash. Since the heavy and light grains are now more nearly of the same size, the lights may be easily suspended and removed, as evidenced by the *CTSV* relationship (ab), thus enriching the deposit even further. If these deposits are now dried out and incorporated by winds into the dunes as would occur after a storm, the dunes also would become enriched (ca).

As has been argued by Hand (1964) and others, the difference in density between air and water causes the heavy/light size ratios for dunes to be larger than those in light layers of waterlaid deposits. Re-erosion of the heavy-enriched dunes by the upper swash will result

in the formation of relatively thick heavy mineral layers. In addition, the coarser quartz may be rolled away because the $R*$ values are below 70, the *BKS* at the top of the swash is more nearly the size of the heavies, and because suspension will select out the lights which are smaller than those which would be the SHE size of the heavies.

This analysis offers an alternative explanation to that of Stapor (1973) who studied the marine, coastal, and dune sands of Apalachicola, Florida. He argued that the "black sands" were deposited as slugs of heavy mineral rich sand from offshore. The enrichment of these slugs was presumably due to more rapid shoreward movement of the finer (more heavy rich fractions) than the coarser. However, the fact that the heavy deposits were found as *high berms,* and the quartz grain size within the heavy layer was smaller than within the light layers indicates precisely those conditions expected for concentration of heavies in the upper swash by the processes indicated in this paper.

SUMMARY

1. A theoretical analysis of fluid flow and sediment properties has led to the development of a critical entrainment and critical suspension velocity equation which allows the prediction of the sizes of heavy and light minerals which will be deposited together in sands. The entrainment critical velocity equation:

$$V_C = 5.75 \log_{10}\left(\frac{30.2xy}{BKS}\right)\beta_1\beta_2$$

$$\sqrt{\frac{4dg \cos \alpha(\rho_p - \rho_f)(\tan \phi - \tan \alpha)}{3C_d\rho_f}}$$

predicts a decrease in critical velocity with decreasing size for single sized sediments from 10 to 0.05 mm. For mixed sizes, the function predicts that depending upon the roughness size of the bed and the size of the particle in question, larger sizes may have lower critical velocities than smaller, and that entrainment equivalent size ratios of heavies to lights may be up to four times smaller than those predicted by the settling laws.

The critical suspension equation:

$$Vcs = 5.75 \log_{10}\left(\frac{30.2xy}{BKS}\right)Vs$$

where Vs is the constant terminal settling velocity in still water, gives the horizontal flow velocity needed to maintain suspension of a particular sized particle and thus allows a direct comparison with entrainment critical velocities.

2. Experimental data show that for sizes 0.05 to 0.8 mm when $d = BKS$ and surface fluid velocities equal about 66 cm/sec, the intermediate sizes (around 0.3 mm) are least easily moved. Thus depending upon the BKS and $R*$ values, the 0.18 mm size is not necessarily the most easily entrainable size. In fact under certain $R*$ conditions and when $BKS < 0.18$, 0.18 mm is the most difficult size to move. Thus the use of generalized Vc size functions such as the Hjulstrom or Inman curves will give erroneous results for sands. For samples of size 0.088 to 0.707 mm on a bed of natural quartz of size 0.22 mm, more of the larger sizes (0.324 to 0.707 mm) are removed than finer for low $R*$ but as $R*$ increases higher amounts of fines are removed. The same occurs with constant flow velocity but increasing BKS.

3. The CTSV relationships of light and heavy minerals in sands may be classified by four combinations of the ratio of median heavy size to bottom roughness size (d/BKS) and the boundary Reynolds number $R*$, as presented in Fig. 10. These may produce $CTSV_h/CTSV_l$ ratios which range from about 0.25 to 2.7.

4. Garnet and quartz mineral sizes for a beach at Presque Isle, Lake Erie, show no statistical size difference for samples from heavy layers as predicted by Fig. 10. The light layers have size ratios predictable by settling theory.

5. A beach size budget based on these results and applied to the Presque Isle beach shows that SHE sizes brought in suspension and entrainment equivalent sizes brought in by bedload will be deposited up the swash with size relationships such that the heavies are concentrated at the top of the swash by Fig. 10 case 1 mechanisms. Incorporation into the dunes of this heavy-rich fine deposit will cause increased heavy concentration in the dunes. The erosion of dunes by water has a high probability of producing large heavy mineral concentrates because 1) the heavy/light $CTSV$ ratios are greater than 1, 2) the dunes have an increased concentration of heavies, and 3) erosion of the dunes by the upper swash provides a favorable BKS-$R*$ combination.

APPLICATIONS

1. These results impose serious restrictions on the use of heavy and light mineral $CTSV$ ratios to indicate the medium of deposition of a sediment. The delta values of Hand (1964) used to differentiate dune (air-settled) from beach (water-settled) sands may reflect entrainment equivalent sizes rather than the different densities of the depositing medium.

2. The location of heavy mineral placer deposits might now be predicted by prospecting for those $R*$-BKS conditions most favorable for heavy mineral enrichment as outlined in Fig. 10. The use of $CTSV$ ratios as illustrated in Lowright et al. (1972) and applied by Pretorius (personal communication), however, is further restricted by the findings of this report. Deviations from SHE are indications not only of distance from source but primarily of hydraulic and boundary roughness conditions.

REFERENCES

BRIGGS, L. I., 1965, Heavy mineral correlations and provenances: Jour. Sed. Petrology, v. 35, no. 4, p. 939–955.

COLEMAN, N. L., 1967, A theoretical and experimental study of drag and lift forces: Int. Assoc. Hydro. Res., 12th Cong., Ft. Collins, Colo.

EINSTEIN, H. A., 1950, The bedload function for sediment transportation in open channel flows: U.S. Dept. of Agriculture Tech. Bull. No. 1026, 71 p.

FENIAK, M. W., 1944, Grain sizes and shapes of various minerals in igneous rocks: Am. Mineralogist, v. 29, p. 415–421.

GRAF, W. H., 1972, Hydraulics of sediment transport: McGraw-Hill, New York, 513 p.

GRASS, A. J., 1970, Initial instability of fine bed sand: ASCE Hydraulics Division, v. 96, p. 619.

———, 1967, The measure of turbulent velocity fluctuations close to a boundary in open channel flow: Proc. 12th IAHR, v. 2, p. 201.

GILBERT, G. K., 1914, The transportation of debris by running water: U.S. Geol. Survey, Prof. Paper 86.

GRIGG, N. S., AND R. E. RATHBUN, 1969, Hydraulic equivalence of minerals with a consideration of the reentrainment process: U.S. Geol. Survey, Prof. Paper 650B, p. B77–B80.

HAND, B. M., 1964, Hydrodynamics of beach and dune sedimentation: unpublished Ph.D. Thesis, Pennsylvania State University, 159 p.

HJULSTROM, F., 1935, Studies of the morphological activity of rivers as illustrated by River Fyris: Bull. Geol. Inst. Upsala, v. 25, Chapt. III.

INMAN, D. L., 1949, Sorting of sediments in the light of fluid mechanics: Jour. Sed. Petrology, v. 19, p. 51–70.

IPPEN, A. T., AND A. S. EAGLESON, 1955, A study of sediment sorting by waves shoaling on a plane beach: MIT Technical Report No. 18.

JAMES, M. L., G. M. SMITH, AND J. C. WOLFORD, 1967, Applied numerical methods for digital computation with Fortran: International Textbook Company, Scranton, Pa., 514 p.

KALINSKE, A. A., 1943, The role of turbulence in river hydraulics: U. of Iowa Studies in Eng. Bull. 27.

LANE, E. W., AND A. A. KALINSKE, 1939, The relation of suspended to bedload material in rivers: Trans. Am. Geophys. Union, v. 20, p. 637–641.

LELIAVSKY, S., 1966, An introduction to fluvial hydraulics: Dover Pub., New York, 257 p.

LOWRIGHT, R., E. G. WILLIAMS, AND F. Dachille, 1972, An analysis of factors controlling deviations in hydraulic equivalence in some modern sands: Jour. Sed. Petrology, v. 42, no. 3, p. 635–645.

MAVIS, F., T. C. HO, AND Y. TU, 1935, The transportation of detritus by flowing water: U. Iowa Studies in Engineering, Bull. 5.

MCINTYRE, D. D., 1959, The hydraulic equivalence and size distributions of some mineral grains from a beach: Jour. Geology, v. 67, no. 3, p. 278–301.

MILLER, R. L., AND R. J. BYRNE, 1966, The angle of repose for a single grain on a fixed rough bed: Sedimentology, v. 6, p. 303–314.

NEVIN, C., 1946, Competancy of moving water to transport debris: Geol. Soc. America Bull., v. 57, p. 651–674.

RITTENHOUSE, G., 1943, The transportation and deposition of heavy minerals: Geol. Soc. America Bull., v. 54, p. 1725–1780.

RUBEY, W. W., 1933, The size distribution of heavy minerals within a water-laid sandstone: Jour. Sed. Petrology, v. 3, p. 3–29.

SHANOV, V. N., 1964, The distribution of minerals in the size fractions of sand de_ osited by water and wind: Universitat, Vestnik Leningradskii 6, p. 155–163.

SLINGERLAND, R. L., 1973, Transportation and hydraulic equivalence relationships of light & heavy minerals in sands: unpublished M.S. Thesis, Pennsylvania State University, 120 p.

STAPOR, F. W., 1973, Heavy mineral concentrating processes and density/shape/size equilibria in the marine and coastal dune sands of the Apalachicola, Fla. region: Jour. Sed. Petrology, v. 43, no. 2, p. 396–407.

SUNDBORG, A., 1956, The River Klaralven; a study in fluvial processes: Geografiska Annaler, Ser. A., no. 115, p. 125–316.

UNITED STATES WATERWAYS EXPERIMENT STATION, Paper # 17 USWES, 1935.

VAN ANDEL, T., 1950, Provenance, transport, and deposition of Rhine River sediments: Doctoral Thesis, University of Groningen.

VON ENGELHARDT, W., 1940, The distinction of water and wind-sorted sands on the basis of the grain-size distribution of their light and heavy components: Chemie der Erde, v. 12, p. 445–465.

WHITE, C., 1940, The equilibrium of grains on the bed of a stream: Proc. Roy. Soc. London, 174-A.

YALIN, M., 1972, Mechanics of sediment transport: Pergamon Press, New York, 290 p.